Proceedings of the 37th Chinese Control Conference
July 25-27, 2018, Wuhan, China

Finite-time Robust Control for Inertially Stabilized Platform Based on Terminal Sliding Mode

GE Suoliang[1], ZHAO Lei[1], PING Zhaowu[1], YANG Shuang[2]

1. School of Electrical Engineering and Automation, Hefei University of Technology, Hefei 230009, P. R. China
E-mail: gesuol@163.com, zhaol429@mail.hfut.edu.cn, zwping@hfut.edu.cn

2. School of Automation, Northwestern Polytechnical University, Xi'an 710129, P. R. China
E-mail: shuangyang@mail.nwpu.edu.cn

Abstract: In this paper, a finite-time robust controller is designed based on the terminal sliding mode for a two-axis gimbal ISP system. It is shown that the controller designed in this paper can not only ensure the system output tracking error converge to zero in a finite time, but also provide a strong disturbance rejection performance. In addition, the gain of the finite-time robust controller can be significantly reduced with respect to the ones of linear sliding mode control schemes as well as PID control methods. Simulation results will also be provided to demonstrate the effectiveness of the designed controller.

Key Words: Inertially Stabilized Platform, Finite-time Robust Control, Terminal Sliding Mode, Finite-time Convergence, Disturbance Rejection

1 Introduction

Recently, the inertially stabilized platform (ISP) is used widely in the modern weapon equipment and civilian infrastructure, especially in the inertial guidance and navigation systems such as ballistic missiles, unmanned aircrafts, spacecrafts and automatic tracking radars, etc. In [1], the basic principles and techniques are introduced. In addition, it analyses diverse structures of ISPs, key design issues and its applications in scientific, military, and commercial zones.

Many researchers at home and abroad have been studying the stabilization control problem for ISP, that is, hold or control the line of sight (LOS) of one object relative to another object or inertial space. In [2], a two-axis yaw-pitch gimbals configuration is discussed, and the equations of motion are derived by the moment equation as well as the Lagrange equations. In [3], a double closed-loop control scheme is proposed to realize the tracking control when the target is highly dynamic or when the imaging sensor is carried on a mobile vehicle. In [4], in order to achieve the pointing-tracking control for dynamic targets, a novel image-based pointing-tracking feedback control scheme is proposed with the enhancement of the intuitive decoupled controller structure by measuring the camera inertial angular rate around its optical axis for an inertial stabilized double-gimbal airborne camera platform combined with a computer vision system. The proportional-integral-derivative (PID) control method is adopted in most ISPs system at present. In [5], for the sake of the settlement of uncertainties, a robust PID controller via linear matrix inequality (LMI) is designed with the employment of multiple-model paradigm. In [6], a robust PID controller is devised based on the system model with a stronger robustness and anti-jamming ability. For time-invariant system, the PID control scheme is extremely effective. However, the ISP is a class of complex nonlinear uncertain systems, which are difficult to obtain the precise model, owing to the factors of torque coupling, load variation, mechanical resonance and electrical parameter fluctuations, etc [1–4]. Therefore, it is hard to get satisfied control effect utilizing the PID method. To reach the goal, some researchers proposed a set of advanced control strategies. In [7], a hybrid control strategy is proposed based on the double compensations of disturbance and speed. The anti-interference ability of the ISP system is enhanced and its control accuracy is improved as well. In [8], a self-tuning control scheme is formulated based on the linear quadratic Gaussian (LQR) algorithm for disturbances resulting from nonlinear phenomena such as Coulomb friction in ISP systems. And it presented a good performance of compensation for nonlinear disturbance and interference immunity as well as robustness.

In order to deal with system uncertainties and external disturbances better, the variable structure control (VSC) method with perfect performance of parameter insensitivity and disturbance rejection is employed. In [9], a VSC scheme is proposed to realize the current control of time optimal and rejection of disturbance for a four-phase switched reluctance motor with the torque ripple and nonlinearity. In [10], a sliding mode control (SMC) method of relatively simple realization is derived with excellent tracking performance in the face of ill-defined disturbance and unknown system parameters. In [11], a grey sliding mode controller is designed to reduce effectively the influence of friction disturbance on the system under the condition of no friction model when the impact of servo tracking performance of friction disturbance on the gyro stabilized platform is considered. In [12], a nonlinear dynamic model based on the geographic coordinate is established for a two-axis ISP. Then, a compound control method based on the back-stepping SMC and the adaptive radial basis function neural network (RBFNN) is proposed. And the back-stepping SMC is proposed to deal with the system nonlinearity, parameter variations, and disturbance. Furthermore, the adaptive RBFNN is constructed and optimized to estimate the upper bound of the residual error on line to reduce the chattering phenomenon of SMC. However, all the sliding mode controllers are designed based on linear sliding mode, which can guarantee only the asymptotic error convergence on the sliding mode and therefore error dynamic can not converge to zero in a finite time. In [13], in order to realize the finite time control, by introducing nonlin-

This work is supported by National Natural Science Foundation (NNSF) of China under Grant 61403117.

ear term in the linear sliding mode, a terminal sliding mode (TSM) control scheme is proposed with the convergence of dynamic error in a finite time. Nonetheless, there exists a singular problem in the TSM controller design mentioned above. In [14], one approach is proposed with switching the sliding mode between TSM and linear hyperplane based sliding to address the singular problem. In [15], by transferring the trajectory to a pre-specified open region where TSM control is not singular, the singularity of TSM is avoided indirectly. In [16], a global non-singular terminal sliding mode (NTSM) controller is designed with the direct elimination of the singularity associated with conventional TSM control via redesigning the TSM manifold. In [17] and [18], two kinds of TSM control schemes are proposed with the finite-time convergence of dynamic error as well as the eliminations of the singularity and the reaching phase of SMC.

In this paper, a finite-time robust (FTR) controller is designed with the finite-time convergence of output error for a two-axis gimbal ISP with parameter uncertainties when the external disturbance is considered. The basic principle of parameter preference is given and the system stability is demonstrated based on the Lyapunov stability theory. Compared with the conventional PID control method, the FTR control approach decreases the influence of parameter uncertainties and external disturbance on the system. Meanwhile, the gain of FTR control can be significantly reduced with respect to the high gain of PID and linear sliding mode controllers and the system robustness is enhanced. Finally, numerical simulations show the expected control performance analyzed above.

The rest of this paper is organized as follows. In Section 2, the two-axis gimbal configuration is briefly analyzed, and the mathematical modeling is formulated. In Section 3, a FTR controller is designed for a single input single output (SISO) system, and the stability of the system is proved based on the Lyapunov stability theory. In Section 4, the numerical simulations are carried out. Section 5 gives the conclusion.

2 Preliminaries and Dynamical Modeling

2.1 Preliminaries

As it can be seen in Fig. 1, the two-axis ISP is composed of two gimbal frames, i.e., the inner pitch gimbal and the outer yaw gimbal, where three reference frames are depicted as follows: a fuselage body-fixed frame B, a frame A fixed to the pitch gimbal, and a frame K fixed to the yaw gimbal. x_k, y_k, z_k and x_a, y_a, z_a are the yaw and pitch gimbal frame axes respectively. x, y, z is the body axis. The x_a-axis coincides with the optimal axis. The positive angle ν_1 is generated by the rotation of body-fixed frame B to the yaw gimbal frame K about the z-axis. The positive angle ν_2 is generated by the rotation of the yaw gimbal frame K to the pitch gimbal frame A about the y_k-axis. For the angular velocities of frames B, K and A, respectively, we introduce the $[p \quad q \quad r]^T$, $[p_k \quad q_k \quad r_k]^T$, $[p_a \quad q_a \quad r_a]^T$, where p, q, r are the components in frame B of the inertial angular velocity vector of the frame B itself, and similarly for the other vectors. And we use the notations p, q, r for the roll, pitch, and yaw components respectively. The relationships between the angular velocities are as follows.

$$\begin{bmatrix} p_k \\ q_k \\ r_k \end{bmatrix} = \begin{bmatrix} cos\nu_1 & sin\nu_1 & 0 \\ -sin\nu_1 & cos\nu_1 & 0 \\ 0 & 0 & 1 \end{bmatrix} \begin{bmatrix} p \\ q \\ r \end{bmatrix} + \begin{bmatrix} 0 \\ 0 \\ \dot{\nu}_1 \end{bmatrix} \quad (1)$$

$$\begin{bmatrix} p_a \\ q_a \\ r_a \end{bmatrix} = \begin{bmatrix} cos\nu_2 & 0 & -sin\nu_2 \\ 0 & 1 & 0 \\ sin\nu_2 & 0 & cos\nu_2 \end{bmatrix} \begin{bmatrix} p_k \\ q_k \\ r_k \end{bmatrix} + \begin{bmatrix} 0 \\ \dot{\nu}_2 \\ 0 \end{bmatrix} \quad (2)$$

Suppose that the body attitude angles, that is, the angles of yaw, pitch, and roll, are ψ, θ, ϕ respectively, then the velocities of body are

$$\begin{bmatrix} p \\ q \\ r \end{bmatrix} = \begin{bmatrix} \dot{\phi} + \dot{\psi} sin\theta \\ \dot{\theta} cos\phi - \dot{\psi} sin\phi cos\theta \\ \dot{\theta} sin\phi + \dot{\psi} cos\phi cos\theta \end{bmatrix} \quad (3)$$

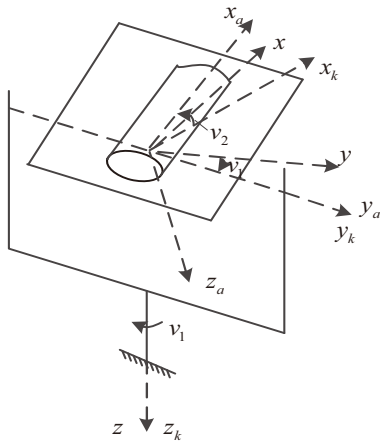

Fig. 1: The two-axis ISP gimbal configuration.

As mentioned above, the two-axis ISP involves the yaw gimbal and the pitch gimbal. Here, the two channels of yaw and pitch are modeled respectively.

2.2 Dynamical modeling of pitch channel

According to Yoon and Lundberg [3], the dynamical equation for the pitch gimbal can be derived as follows based on the Goth rotation theorem and momentum theorem:

$$\begin{aligned} I_{ay}\dot{q}_a =& T_y + (I_{az} - I_{ax})p_a r_a + D_{xz}(p_a^2 - r_a^2) \\ & - D_{yz}(\dot{r}_a - p_a q_a) - D_{xy}(\dot{p}_a + q_a r_a) \end{aligned} \quad (4)$$

where T_y is the external torque applied to the pitch gimbal y_a-axis. $I_{(\cdot)}$ and $D_{(\cdot)}$ are the moment of inertia as well as product of inertia of the body, respectively. The block diagram for the pitch channel is shown in Fig. 2, where α is the azimuth angle of pitch gimbal. T_D can be regarded as the disturbance term of the pitch gimbal, which includes the interference moment caused by the body rotations, the cross coupling interference moment caused by the yaw gimbal to the pitch gimbal and the external disturbance torque.

2.3 Dynamical modeling of yaw channel

As depicted in [3], the following equation of motion can be derived for the yaw gimbal:

$$\Phi_k \dot{r}_k = T_z + T_{d1} + T_{d2} + T_{d3} \quad (5)$$

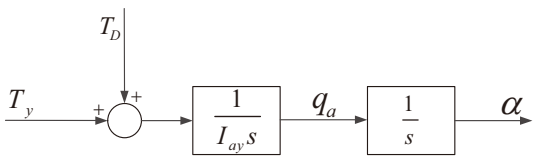

Fig. 2: The block diagram of pitch channel.

with

$$\begin{aligned}
\Phi_k &= I_{kz} + I_{ax}sin^2\nu_2 + I_{az}cos^2\nu_2 - D_{xz}sin(2\nu_2)\\
T_{d1} &= [I_{kx} + I_{ax}cos^2\nu_2 + I_{az}sin^2\nu_2 + D_{xz}sin(2\nu_2)\\
&\quad - (I_{ky} + I_{ay})]p_kq_k\\
T_{d2} &= -[d_{xz} + (I_{az} - I_{ax})sin\nu_2cos\nu_2 + D_{xz}cos(2\nu_2)]\\
&\quad \times (\dot{p}_k - q_kr_k) - (d_{yz} + D_{yz}cos\nu_2 - D_{xy}sin\nu_2)\\
&\quad \times (\dot{q}_k + p_kr_k) - (d_{xy} + D_{xy}cos\nu_2 + D_{yz}sin\nu_2)\\
&\quad \times (p_k^2 - q_k^2)\\
T_{d3} &= \ddot{\nu}_2(D_{xy}sin\nu_2 - D_{yz}cos\nu_2) + \dot{\nu}_2[(I_{ax} - I_{az})(p_k\\
&\quad \times cos(2\nu_2) - r_ksin(2\nu_2)) + 2D_{xz}(p_ksin(2\nu_2)\\
&\quad + r_kcos(2\nu_2)) + (D_{yz}sin\nu_2 + D_{xy}cos\nu_2)\\
&\quad \times (q_a + q_k) - I_{ay}p_k]
\end{aligned}$$

where Φ_k is the total moment of inertia about the yaw gimbal z_k-axis and $d_{(\cdot)}$ is the product of inertia of the body. T_{d1}, T_{d2}, and T_{d3} represent different gimbal inertia disturbances. The block diagram for the yaw channel is shown in Fig. 3, where β is the pitch angle of pitch gimbal, T_z is the external torque applied to the yaw gimbal z_k-axis. $T_d = T_{d1} + T_{d2} + T_{d3}$ can be treated as the disturbance term of the yaw gimbal including the disturbance moment caused by the body rotation, the cross coupling interference moment caused by the pitch gimbal to the yaw gimbal and the external interference torque.

3 Design of Finite-Time Robust Controller

In order to realize the finite-time control, there are usually three kinds of design methods, i.e., the homogeneous theory-based method, adding a power integrator-based method, and terminal sliding mode-based method. Here, in this paper, we use terminal sliding mode-based method to design a FTR controller for ISP. By inserting nonlinear terms in the linear sliding mode, the TSM is developed and the control law is designed through suitable parameter choice of the TSM. The controller can ensure the finite-time convergence of tracking error and the avoidance of singularity of conventional TSM.

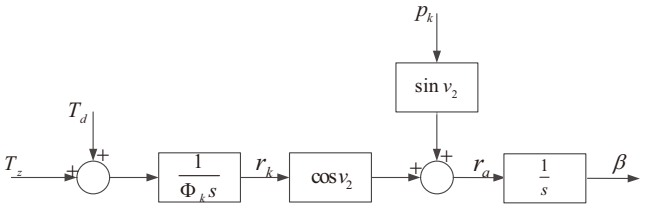

Fig. 3: The block diagram of yaw channel.

Consider the following n-order SISO system

$$\begin{aligned}
\dot{x}_k &= x_{k+1}, \quad (k = 1, 2, \ldots, n-1)\\
\dot{x}_n &= f(x,t) + \Delta f(x,t) + b(x,t)u(t) + d(x,t) \quad (6)
\end{aligned}$$

where $x_1 = y, \ldots, x_n = y^{(n-1)}$, y is the system output, $f(x,t)$ is the known nonlinear term for the system, $b(x,t)$ is the system input coefficient, $u(t)$ is the system control input, $\Delta f(x,t)$ and $d(x,t)$ are the unknown uncertainties and external disturbance, respectively. And they satisfy the following bounded condition

$$|\Delta f(x,t)| \le \Psi(x,t) \quad (7)$$

$$|d(x,t)| \le B(x,t) \quad (8)$$

where $\Psi(x,t)$ and $B(x,t)$ are both non-negative functions.

The terminal sliding-mode manifold is selected as follows:

$$\gamma(x,t) = \boldsymbol{\Lambda E}(t) - \boldsymbol{\Lambda Z}(t) \quad (9)$$

where $\boldsymbol{\Lambda} = [\Lambda_1, \ldots, \Lambda_n]$, $\Lambda_i (i = 1, 2, \ldots, n)$ is a positive constant, and it satisfies the criterion i), $\boldsymbol{E}(t) = [e\ \dot{e}\ \ldots\ e^{(n-1)}]^T$ is the error vector. $e = x_o - x_{od}$, where x_o is the actual output of the system, x_{od} is the desired output. $\boldsymbol{Z}(t) = [z(t)\ \dot{z}(t)\ \ldots\ z^{(n-1)}(t)]^T$, and $z(t)$ satisfies the criteria ii) and iii).

i). The eigenvalues of equation $\Lambda_n s^{n-1} + \Lambda_{n-1}s^{n-2} + \cdots + \Lambda_1 = 0$ are all in the left half of s plane.

ii). $z(t)$ is a n-order differentiable continuous function in the section of $[0, \infty)$.

iii). For a constant $T > 0$, $z(t)$ is bounded in the period of $[0, T]$, and and satisfies that $z(0) = e(0), \dot{z}(0) = \dot{e}(0), \ldots, z^{(n)}(0) = e^{(n)}(0)$.

Assume that $z(t)$ is selected as follows

$$z(t) = \begin{cases} a_0 + \sum\limits_{i=1}^{2n+1} a_i t^i, & if\ 0 \le t \le T \\ 0, & if\ t > T \end{cases} \quad (10)$$

then, according to ii) and iii), $z(t)$ satisfies that

$$z(0) = e(0), \dot{z}(0) = \dot{e}(0), \ldots, z^{(n)}(0) = e^{(n)}(0) \quad (11)$$

$$z(T) = e(T), \dot{z}(T) = \dot{e}(T), \ldots, z^{(n)}(T) = e^{(n)}(T) \quad (12)$$

the parameter a_i can be determined by the formula (11) and (12). In addition, according to (9) and iii), $\gamma(x,0) = \boldsymbol{\Lambda E}(0) - \boldsymbol{\Lambda Z}(0) = 0$ is confirmed, i.e., the initial state of system is on the sliding mode manifold, that is, the reaching phase of SMC is eliminated.

Since the initial state is already on the sliding mode manifold, it is necessary to design a control law to maintain the state and drive it to the equilibrium point in a finite time. According to the selected sliding mode manifold for system (6), a FTR controller is designed as follows.

Theorem 1 *For the n-order SISO nonlinear system (6), according to the sliding mode manifold (9), if the control input is designed as follows:*

$$\begin{aligned}
u(t) = &-\frac{1}{b(x,t)}\{f(x,t) - x_{1d}^{(n)} - z^{(n)}(t)\\
&+ \frac{1}{\Lambda_n}\sum_{j=1}^{n-1}\Lambda_j(e^{(j)} - z^{(j)}(t))\\
&+ \frac{\gamma(x,t)\Lambda_n}{|\gamma(x,t)\Lambda_n|}[\Psi(x,t) + B(x,t) + \eta]\}
\end{aligned} \quad (13)$$

then the system state can converge to equilibrium point in a finite time, where η is a positive constant.

Proof. A candidate Lyapunov function for system (6) is chosen as follows:

$$S = \frac{1}{2}\gamma^2(x,t) \tag{14}$$

differentiating (14) with respect to time, one can obtain that

$$\begin{aligned}
\dot{S} &= \gamma\dot{\gamma} = \gamma(x,t)[\boldsymbol{\Lambda}\dot{\boldsymbol{E}}(x,t) - \boldsymbol{\Lambda}\dot{\boldsymbol{Z}}(x,t)] \\
&= \gamma(x,t)\{\boldsymbol{\Lambda}[\dot{e} \quad \ddot{e} \quad \dots \quad e^{(n)}]^T \\
&\quad - \boldsymbol{\Lambda}[\dot{z}(t) \quad \ddot{z}(t) \quad \dots \quad z^{(n)}(t)]^T\} \\
&= \gamma(x,t)\{\Lambda_n[e^{(n)} - z^{(n)}(t)] \\
&\quad + \sum_{j=1}^{n-1}\Lambda_j[e^{(j)} - z^{(j)}(t)]\} \\
&= \gamma(x,t)\{\Lambda_n[x_o^{(n)} - x_{od}^{(n)} - z^{(n)}(t)] \\
&\quad + \sum_{j=1}^{n-1}\Lambda_j[e^{(j)} - z^{(j)}(t)]\} \\
&= \gamma(x,t)\{\Lambda_n[f(x,t) + \Delta f(x,t) \\
&\quad + b(x,t)u(t) + d(x,t) - x_{od}^{(n)} \\
&\quad - z^{(n)}(t)] + \sum_{j=1}^{n-1}\Lambda_j[e^{(j)} - z^{(j)}(t)]\}
\end{aligned} \tag{15}$$

substitute (13) into equation (15), it is obtained that

$$\begin{aligned}
\dot{S} &= \gamma(x,t)\Lambda_n\{[\Delta f(x,t) + d(x,t)] \\
&\quad - \frac{\gamma(x,t)\Lambda_n}{|\gamma(x,t)\Lambda_n|}[\Psi(x,t) + B(x,t) + \eta]\}
\end{aligned} \tag{16}$$

according to (7) and (8), one can conclude that

$$\begin{aligned}
\dot{S} &\le |\gamma(x,t)\Lambda_n||\Delta f(x,t) + d(x,t)| \\
&\quad - |\gamma(x,t)\Lambda_n|[\Psi(x,t) + B(x,t) + \eta] \\
&\le -\eta|\gamma(x,t)\Lambda_n| < 0 \quad (|\gamma(x,t)\Lambda_n| \neq 0).
\end{aligned} \tag{17}$$

Based on the Lyapunov stability theory, one can conclude from (14) and (17) that the designed control law can stabilize the system state on the sliding mode manifold. In addition, when $t > T$, on the basis of (12) and ii), one can obtain that $\boldsymbol{Z}(t) = 0$, i.e., $z(t) = \dot{z}(t) = \cdots = z^{(n-1)}(t) = 0$.

Meanwhile, because there is $\gamma(x,t) = 0$, one can obtain that

$$\Lambda_n e^{(n-1)} + \Lambda_{n-1}e^{(n-2)} + \cdots + \Lambda_1 e = 0 \tag{18}$$

according to (18) and i), $e = 0$ is obtained, i.e., the output error of system is zero when $t > T$. And one can conclude that the system state can converge to equilibrium point in a finite time T. To sum up, the control scheme designed in *theorem 1* can realize the global robustness and system stability for the ISP.

Because the term $\frac{\gamma(x,t)\Lambda_n}{|\gamma(x,t)\Lambda_n|}$ in expression (13) is discontinuous, which may cause chatterings for the system, it is necessary to overcome them. To eliminate the effects of the chatterings, one can use the following term in place of the discontinuous term in expression (13)

$$\Theta = \frac{\gamma(x,t)\Lambda_n}{|\gamma(x,t)\Lambda_n| + \delta_0 + \delta_1|e|} \tag{19}$$

where δ_0 and δ_1 are both positive constants.

4 Simulation Results

In order to verify the effectiveness of the FTR control scheme designed in this paper, the numerical simulation is conducted for a two-axis gimbal ISP with its configuration parameters in Table 1. Considering the influence of cross coupling between channels is less significant, so it can be designed according to single channel.

Table 1: The two-axis ISP configuration parameters

Parameter	Value	Unit
I_{ax}	0.0168	Nms^2/rad
I_{ay}	0.0168	Nms^2/rad
I_{az}	0.0168	Nms^2/rad
I_{kx}	0.0231	Nms^2/rad
I_{ky}	0.0231	Nms^2/rad
I_{kz}	0.0231	Nms^2/rad

For the model of the two-axis gimbal ISP, assume that the rotation angle of gimbals is $\nu_1 = \nu_2 = 0.1rad$, and the body attitude angle is $\psi = \theta = \phi = 0.5sin(\pi t/3)rad$. The initial state is set as $[x_{1p} \quad x_{2p}]^T = [0.3 \quad 0]^T$, $[x_{1y} \quad x_{2y}]^T = [-0.4 \quad 0]^T$.

For the FTR controller designed in this paper, the controller parameters are set as follows: $a_0 = e(0), a_1 = \dot{e}(0)$, $a_2 = \frac{1}{2}\ddot{e}(0)$, $a_3 = -\frac{10}{T^3}e(0) - \frac{6}{T^2}\dot{e}(0) - \frac{3}{2T}\ddot{e}(0)$, $a_4 = \frac{15}{T^4}e(0) + \frac{8}{T^3}\dot{e}(0) + \frac{3}{2T^2}\ddot{e}(0)$, $a_5 = -\frac{6}{T^5}e(0) - \frac{3}{T^4}\dot{e}(0) - \frac{1}{2T^3}\ddot{e}(0)$, $\boldsymbol{\Lambda} = [25 \quad 1]$, $T = 0.1$, $\eta = 20$, $\Psi(x,t) = 2.0$, $B(x,t) = 30$, $\delta_0 = 0.05$, $\delta_1 = 5.0$.

To have a comparison, two kinds of control algorithms are employed, i.e., one is the designed FTR control algorithm, the other one is the PID control algorithm, which is discussed above.

4.1 The case in the absence of disturbance

The response curves of the pitch and yaw channels under the FTR controller and PID controller in the absence of disturbance are shown in Fig. 4 and 5. The control input curves for them are shown in Fig. 6 and 7.

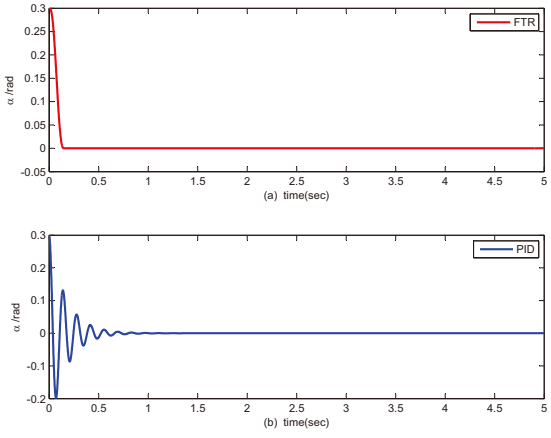

Fig. 4: Response curves of the pitch channel under two kinds of controllers in the absence of disturbance.

4.2 The case in the presence of disturbance

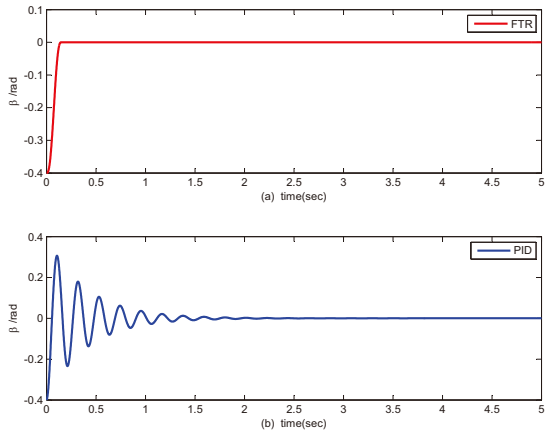

Fig. 5: Response curves of the yaw channel under two kinds of controllers in the absence of disturbance.

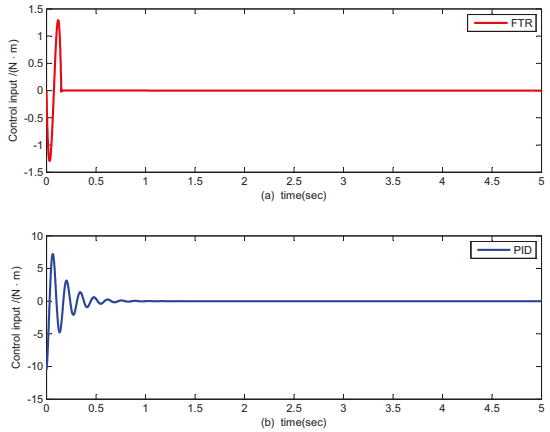

Fig. 6: Control input curves of the pitch channel under two kinds of controllers in the absence of disturbance.

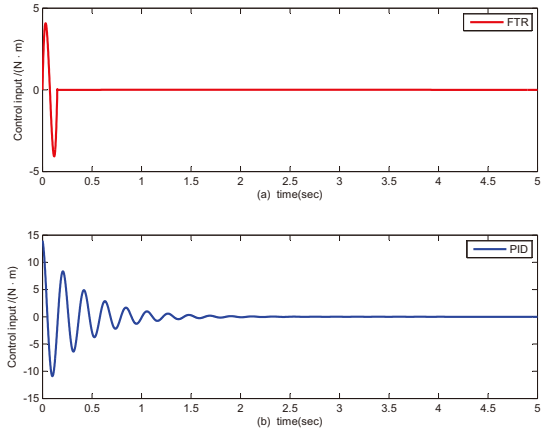

Fig. 7: Control input curves of the yaw channel under two kinds of controllers in the absence of disturbance.

When there is an external disturbance, such as the wind or friction nonlinear disturbance, the disturbance signal directly acts on the ISP's control torque channel. Assume that there is the following disturbance:$d_p(x,t) = 8sin(4\pi t)$, $d_y(x,t) = 10sin(5\pi t)$. The response curves of the ISP system under two kinds of control methods in the presence of disturbance are shown in Figs. 8 and 9.

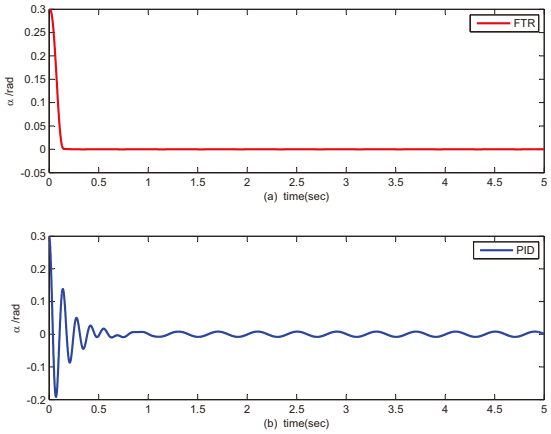

Fig. 8: Response curves of the pitch channel under two kinds of controllers in the presence of disturbance.

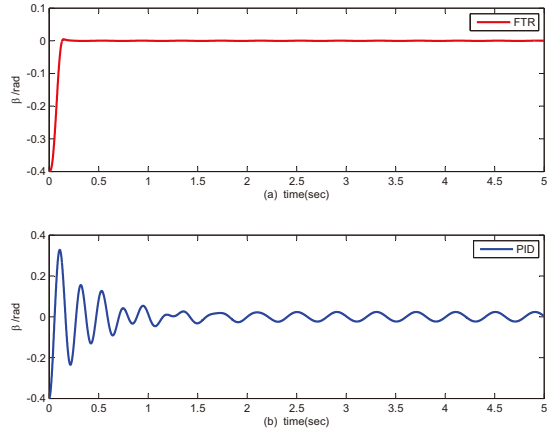

Fig. 9: Response curves of the yaw channel under two kinds of controllers in the presence of disturbance.

It can be seen apparently from the results that the FTR controller designed in this paper offers a better convergence rate and a stronger disturbance rejection performance than the PID control schemes, which have a obvious oscillation process before reaching the stable state. Moreover, the controller gain of the FTR controller is significantly reduced with respect to the ones of PID control methods as well as the linear sliding mode control schemes.

5 Conclusion

In this paper, a two-axis pitch-yaw gimbal ISP is studied. By rebuilding the sliding-mode manifold, a finite-time robust controller is designed for the system. The control scheme developed in this paper not only makes sure the system output tracking dynamic error can converge to zero in a finite time which can be set arbitrarily, but also offers a stronger disturbance rejection performance than PID control methods. Furthermore, compared with the PID controller, the control gain of the finite-time robust controller

can be significantly reduced, which is friendly for the actuators. The simulation results have verified the excellent performance of the designed controller. The further work on designing a sliding mode-based adaptive controller and the sliding mode observer-based diagnosis system are under the authors' investigation.

References

[1] J. Hilkert, Inertially stabilized platform technology: Concepts and principles. *IEEE Control Systems*, 28(1): 26-46, 2008.

[2] Y. Yoon, J. Lundberg, Equations of motion for a two axes gimbal system. *IEEE Trans. on Aerospace and Electronic Systems*, 37(3): 1083-1091, 2001.

[3] M. Masten, Inertially stabilized platforms for optical imaging systems. *IEEE Control Systems Magazine*, 28(1): 47-64, 2008.

[4] Z. Hurak, M. Rezac, Image-based pointing and tracking for inertial stabilized airborne camera platform. *IEEE Trans. on Control Systems Technology*, 20(5): 1146-1159, 2012.

[5] M. Ge, M. Chiu, Q. Wang, Robust PID controller design via LMI approach. *Journal of Process Control*, 12(1): 3-13, 2002.

[6] P. Song, Robust control of gyro stabilized platform driven by ultrasonic motor. *Sensors and Actuators A Physical*, 261: 280-287, 2017.

[7] H. Lin, X. Xu, Disturbance and velocity compensation control of carrier roll stabilized platform. *Electric Machines and Control*, 17(11): 83-88, 2013.

[8] B. Li, D. Hullender, Self-tuning controller for nonlinear inertial stabilization systems. *IEEE Trans. on Control Systems Technology*, 6(3): 428-434, 1998.

[9] C. Chiu, H. Lin, R. Lin, W. Su, A VSC approach to minimum-time optimal current control of a switched reluctance motor. *IEEE International Conference on Systems, Man and Cybernetics*, 6: 4580-4584, 2006

[10] B. Smith, W. Schrenk, W. Gass, Y. Shtessel, Sliding mode control in a two-axis gimbal system. *Aerospace Conference*, 5(5): 457-470, 1999.

[11] P. Yang, Q. Li, Nonlinear friction grey sliding mode control for gyro stabilized platform. *Systems Eegineering and Electronics*, 30(7): 1328-1332, 2008.

[12] F. Dong, X. Lei, W. Chou, A dynamic model and control method for a two-axis inertially stabilized platform. *IEEE Trans. on Industrial Electronics*, 64(1): 432-439, 2016.

[13] Z. Man, A. Paplinski, H. Wu, A robust MIMO terminal sliding mode control scheme for rigid robotic manipulators. *IEEE Trans. on Automatic Control*, 39(12): 2464-2469, 1994.

[14] Z. Man, X. Yu, Terminal sliding mode control of MIMO linear systems. *IEEE Trans. On Circuits and Systems-I: Fundamental Theory and Applications*, 44(11): 1065-1070, 1997.

[15] Y. Wu, X. Yu, Z. Man, Terminal slidingmode control design-for uncertain dynamic systems. *Systems and Control Letters*, 34(5): 281-287, 1998.

[16] Y. Feng, X. Yu, Z. Man, Non-singular terminal sliding mode control of rigid manipulators. *Automatica*, 38(12): 2159-2167, 2002.

[17] K. Park, T. Tsuji, Terminal sliding mode control of second-order nonlinear uncertain systems. *International Journal of Robust and Nonlinear Control*, 9(11): 769-780, 2015.

[18] C. Chiu, Derivative and integral terminal sliding mode control for a class of MIMO nonlinear systems. *Automatica*, 48(2): 316-326, 2012.